Eur. Phys. J. A **18**, 421–424 (2003)
DOI 10.1140/epja/i2002-10250-2

THE EUROPEAN PHYSICAL JOURNAL A

ηN final-state interaction in incoherent photoproduction of η-mesons from the deuteron

S. Schneider[1,a], A. Sibirtsev[1], Ch. Elster[1,2], J. Haidenbauer[1], S. Krewald[1], and J. Speth[1]

[1] Institut für Kernphysik, Forschungszentrum Jülich, D-52425 Jülich, Germany
[2] Institute of Nuclear and Particle Physics, Ohio University, Athens, OH 45701, USA

Received: 30 September 2002 /
Published online: 22 October 2003 –

Abstract. An analysis of incoherent photoproduction of η-mesons from the deuteron is presented. We concentrate here on the threshold region. The dominant contribution, the γN-ηN amplitude is described within an isobar model. Effects of the final-state interaction in the NN as well as the ηN systems are included by employing models derived within a meson-exchange approach.

PACS. 13.60.Le Meson production – 13.75.Cs Nucleon-nucleon interactions (including antinucleons, deuterons, etc.) – 14.40.Aq Π, K, and η mesons

1 Introduction

The incoherent photoproduction of η-mesons from the deuteron near threshold offers an opportunity to gain insight into the final-state interactions between the outgoing nucleons and the η-meson. Measurements by the TAPS Collaboration [1,2] at MAMI on photoproduction of η-mesons from ^{2}H and ^{4}He show an enhancement in the total cross-sections close to the reaction threshold. Such a threshold enhancement was also observed in π, η, η' and ω production in NN collisions at IUCF, COSY and CELSIUS [3–7]. With the exception of η production, this threshold enhancement could be well described by theoretical calculations including the NN final-state interaction [6,7]. For the η production, also the ηN final-state interaction could play a role [4].

Our knowledge of the ηN interaction is rather poor. Values of the scattering length have been extracted from reactions like $\pi N \to \eta N$ and $\gamma N \to \eta N$. Their real parts range from 0.25 fm to 1.05 fm, as indicated in fig. 1. It is important to study a wider class of η production reactions in order to see to what extent predicted values are compatible with each other.

We now investigate the effect of the ηN interaction in the reaction $\gamma d \to np\eta$. We take into account the lowest-order contributions of the scattering series: the impulse approximation and the NN and ηN final-state interactions.

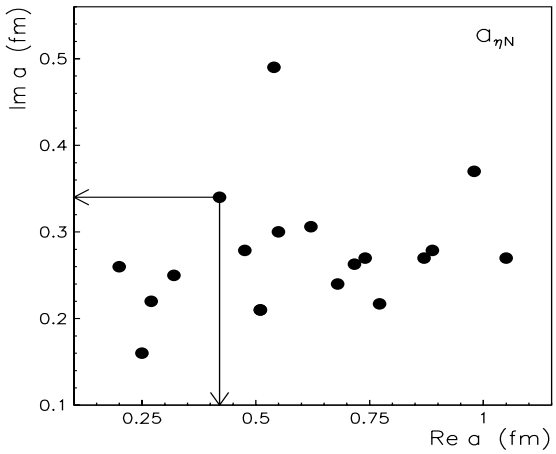

Fig. 1. The real and imaginary parts of the ηN scattering length as reviewed in [8]. The arrows indicate the value employed in our work.

2 The reaction $\gamma d \to np\eta$

The photoproduction amplitude for η-mesons on a single nucleon is described within an isobar model. We only consider the dominant contribution via excitation of the $S_{11}(1535)$-resonance, since other contributions as from t-channel vector meson exchange and the nucleon pole graph were found to be negligible [9,10]. Details of the production mechanism can be found in ref. [11].

For the reaction $\gamma d \to np\eta$ the amplitude $\mathcal{M}_{\rm IA}$ of the impulse approximation can be written as

$$\mathcal{M}_{\rm IA} = A^T(s_1)\Phi(p_2) - (-1)^{S+T}A^T(s_2)\Phi(p_1). \quad (1)$$

[a] e-mail: s.schneider@fz-juelich.de

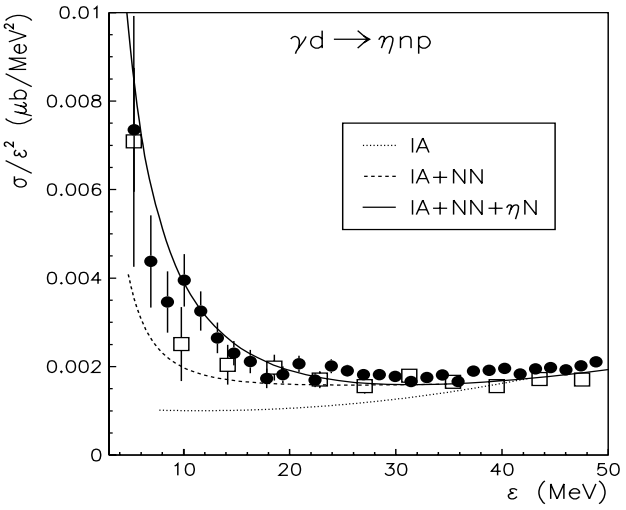

Fig. 2. The total cross-sections divided by ϵ^2 for incoherent η photoproduction off the deuteron as a function of the excess energy ϵ. The dotted line shows the impulse approximation, the dashed line results from inclusion of the NN final-state interaction, and the solid line shows the full calculation, including in addition the ηN final-state interaction. The data are from refs. [1] (squares) and [2] (circles).

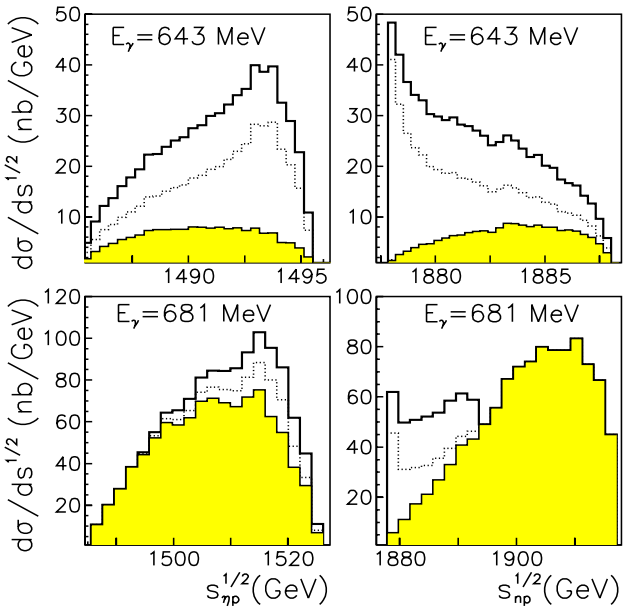

Fig. 3. The invariant-mass spectra of the ηp and the np systems in the reaction $\gamma d \to np\eta$. The shaded areas show the results for the impulse approximation, the dashed line was calculated by including also the np final-state interaction, while the solid line represents the full calculation including np and ηN FSI.

Here, S and T denote the spin and isospin of the outgoing two-nucleon system, $\Phi(p_i)$ stands for the deuteron wave function, p_1 and p_2 are the momenta of the proton or neutron in the deuteron rest frame, and $A^T(s_i)$ gives the η-meson photoproduction amplitude at the invariant collision energy of the corresponding γ-nucleon system.

In the next order of the scattering series, the final-state interaction between the two nucleons and between the η and a nucleon have to be accounted for. The np scattering matrix in the $^1S_0$ and $^3S_1$ partial waves was taken from the CD-Bonn potential [12]. However, it should be pointed out that the use of other realistic NN potentials did not have any observable effect on the results. This is not too surprising, for the deuteron wave function falls off rapidly with increasing momentum. Thus it cuts off contributions from higher off-shell momenta in the intermediate NN state, for which the differences in the various NN models are most pronounced.

Finally, to obtain the ηN scattering amplitude in the S_{11} partial wave, we employ the Jülich coupled-channel meson-exchange model developed for πN scattering [13].

The results for the total cross-sections of the reaction $\gamma d \to np\eta$ are shown in fig. 2. Here we divide our calculations and the data by the square of the excess energy, $\epsilon = \sqrt{s} - m_n - m_p - m_\eta$, since the phase space is proportional to ϵ^2. This representation is more illustrative when considering deviations from the energy dependence of the phase space. While the agreement of the calculation within the impulse approximation (dotted line) with the data is quite good for excess energies $\epsilon > 40\,\mathrm{MeV}$, in the threshold region we observe a sizeable underestimation.

The inclusion of the np and ηN FSI in the s-waves leads to an enhancement in the threshold region while it has no effect for $\epsilon > 40\,\mathrm{MeV}$. The results of the full calculation (solid line) are in good agreement with the data.

It may be instructive to study the interplay between the impulse approximation and the final-state interactions more closely. In fig. 3 we present the calculated mass spectra in the ηp and np system, respectively. The shaded areas stand for the invariant-mass distributions resulting from the impulse approximation alone, the dashed lines show the results including the np final-state interaction, and the solid lines show the results of the full calculation.

The full calculation differs from the impulse approximation not only in size, but also in shape. For the lower photon energy, $E_\gamma = 643\,\mathrm{MeV}$, the inclusion of np FSI enhances the cross-section substantially, especially for small np invariant masses. This forces the cross-section also to peak at higher ηp invariant masses. The inclusion of the ηN FSI in addition does not change the shape of both distributions but leads to an overall enhancement. At $E_\gamma = 681\,\mathrm{MeV}$, the shape of the ηp mass distribution is similar to that at $E_\gamma = 643\,\mathrm{MeV}$. The np system shows a double-peak structure with a pronounced peak at high invariant masses coming from the impulse approximation and a structure at low invariant masses which is due to the NN and ηN final-state interactions. The observation of such a double-peak structure could serve as direct evidence of the presence of FSI effects. It should be mentioned that the analysis of the reaction $pp \to pp\eta$ measured at COSY [14] shows quite a similar structure in the pp invariant-mass spectra.

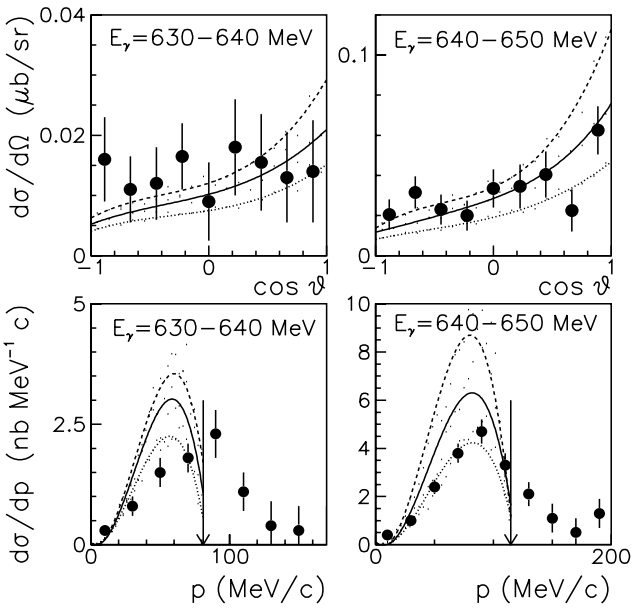

Fig. 4. The angular (upper part) and momentum (lower part) distributions of the η-meson in the γd center-of-mass system. The lines show our calculations with different scattering lengths: $a_{\eta N} = 0.42 + i0.32$ (solid), $0.74 + i0.27$ (dashed) and $0.25 + i0.16$ fm (dotted). The data are from ref. [2]. The arrows show the kinematical limit for η-meson momenta.

It is interesting to investigate to what extent our results depend on the properties of the ηN interaction employed. In [8] we found that the amplitude calculated with the ηN t-matrix from the full model is numerically identical to the amplitude obtained from an effective range expansion of the same t-matrix,

$$\left[iq - \frac{1}{a_{\eta N}}\right]^{-1} = \pi \frac{\sqrt{q^2+{m_N}^2}\sqrt{q^2+{m_\eta}^2}}{\sqrt{q^2+{m_N}^2}+\sqrt{q^2+{m_\eta}^2}} t_{\eta N}(q,q), \quad (2)$$

where q is the on-shell momentum of the η-meson in the ηN center-of-mass system. This can be explained through the good description of the (on-shell) ηN scattering matrix by the effective range expansion up to $q \approx 350$ MeV, as well as through the weak dependence of the half-shell ηN t-matrix on the off-shell momentum. The scattering length $a_{\eta N}$ calculated from the Jülich πN model is

$$a_{\eta N} = 0.42 + i0.34\,\text{fm}\,. \quad (3)$$

This lies roughly in the mid-range of the values for $a_{\eta N}$ given in the literature spreading from $0.25 + i0.16$ fm to $1.05 + i0.27$ fm.

Since we found the effective range expansion to give the same results for the ηN amplitude as the full calculation with the Jülich model, we can now investigate the influence of the strength of the low-energy ηN interaction on the observables of the reaction $\gamma d \to np\eta$. Figure 4 shows the angular and momentum distributions of the η-meson in the threshold region, together with our calculations for $a_{\eta N} = 0.42 + i0.34$ fm (solid line), $a_{\eta N} = 0.25 + i0.16$ fm [15] (dotted line) and $a_{\eta N} = 0.74 + i0.27$ fm [16] (dashed line). In order to make the theoretical predictions comparable to experiment, the result of the calculation was averaged over the energy bins. For the momentum distributions, the arrows indicate the maximum of the kinematically allowed momenta of the η-meson for the maximal photon energy in the energy bin. In the shown momentum spectra, a substantial fraction of the data lies above this limit, indicating perhaps a larger experimental uncertainty in the determination of the η momentum. Unfortunately, we can thus not make a clean comparison between our results and the data. However, we can observe that the data show a preference for smaller values of the ηN scattering length.

3 Conclusion

We calculated total and differential cross-sections for the reaction $\gamma d \to np\eta$ taking into account the dominant contribution from the $S_{11}(1535)$-resonance in the production amplitude as well as the final-state interactions in the NN and ηN systems. FSI effects enhance the cross-sections close to the reaction threshold, at higher energies they have no influence. The Dalitz plots show an enhancement at low invariant masses of the np subsystem due to the inclusion of final-state interaction. At $E_\gamma = 681$ MeV this enhancement leads to a double-peak structure. The experimental observation of such a structure could serve as direct evidence for the presence of FSI effects.

We found that the uncertainty of our calculation is dominated by the uncertainty in the value of the ηN scattering length $a_{\eta N}$. For our calculation we employed the Jülich meson-baryon model and found our results to be compatible with the data. The data taken in the threshold region show a sensitivity to the size of $a_{\eta N}$ and favour smaller values for the real part of the scattering length.

References

1. B. Krusche *et al.*, Phys. Lett. B **358**, 40 (1995).
2. V. Hejny *et al.*, Eur. Phys. J. A **13**, 493 (2002).
3. H.O. Meyer *et al.*, Phys. Rev. Lett. **65**, 2846 (1990); H.O. Meyer *et al.*, Nucl. Phys. A **539**, 633 (1992).
4. H. Calén *et al.*, Phys. Lett. B **366**, 39 (1996); H. Calén *et al.*, Phys. Rev. Lett. **80**, 2069 (1998).
5. P. Moskal *et al.*, Phys. Rev. Lett. **80**, 3202 (1998); P. Moskal *et al.*, Phys. Lett. B **474**, 416 (2000).
6. P. Moskal *et al.*, Phys. Lett. B **482**, 356 (2000).
7. For an overview and further references see, *e.g.*, H. Machner, J. Haidenbauer, J. Phys. G **25**, R231 (1999).
8. A. Sibirtsev, S. Schneider, Ch. Elster, J. Haidenbauer, S. Krewald, J. Speth, Phys. Rev. C **65**, 044007 (2002).
9. G. Knöchlein, D. Drechsel, L. Tiator, Z. Phys. A **352**, 327 (1995).
10. M. Benmerrouche, N.C. Mukhopadhyay, Phys. Rev. D **51**, 3237 (1995).

11. A. Sibirtsev, Ch. Elster, J. Haidenbauer, J. Speth, Phys. Rev. C **64**, 024006 (2001).
12. R. Machleidt, Phys. Rev. C **63**, 024001 (2001).
13. O. Krehl, C. Hanhart, S. Krewald, J. Speth, Phys. Rev. C **62**, 025207 (2000).
14. E. Roderburg and the TOF Collaboration, IKP/COSY Annual Report 2001.
15. C. Bennhold, H. Tanabe, Nucl. Phys. A **530**, 625 (1991).
16. A.M. Green, S. Wycech, Phys. Rev. C **55**, R2167 (1997).